



Title	Nonrelativistic Heavy Quarkonium Model Descended from a Quasi-Particle Approach
Author(s)	Sakai, M.; Hirano, M.; Kat , K.; Matsuda, Y.
Citation	Few-Body Systems, 64(1), 2 https://doi.org/10.1007/s00601-022-01782-w
Issue Date	2023-03
Doc URL	http://hdl.handle.net/2115/91233
Rights	This is a post-peer-review, pre-copyedit version of an article published in Few-body systems. The final authenticated version is available online at: https://doi.org/10.1007/s00601-022-01782-w
Type	article (author version)
File Information	Few-Body Syst 64.pdf



[Instructions for use](#)

Nonrelativistic Heavy Quarkonium Model descended from a Quasi-Particle Approach

M. Sakai^{1,3*}, M. Hirano^{1,3**}, K. Katō^{2,3***} and Y. Matsuda^{3†}

¹ Hokkaido University of Education, Sapporo 002-8502, Japan

² Nuclear Reaction Data Centre, Faculty of Science, Hokkaido University, Sapporo 060-0810, Japan

³ Hokkaido Hadron Study Association, Sapporo 005-0861, Japan

Abstract. A Schrödinger-type equation for a heavy quarkonium in terms of the dynamical quark mass is obtained in a quasi-particle (QP) approach by Llanes-Estrada and Cotanch. To observe the relationship between the obtained equation and the constituent quark (potential) model equation, we treat the dynamical quark mass by a constant parameter M and expand the equation in $1/M$ up to order $(1/M)$. The equation reduces to that of the traditional nonrelativistic constituent quark(CQ) model when a nonlocal interaction is neglected. We investigate the nonrelativistic model where the dynamical quark mass M in the Schrödinger-type equation is treated as a free parameter and call it the quasi-quark (QQ) model. To elucidate the role of the nonlocal interaction and to observe the reliability of the QQ model, we studied the charmonium S -wave states.

1 Introduction

Since the quark model was proposed in 1964, the nonrelativistic constituent quark model has played a pioneering role in the history of hadron research by treating quarks as real dynamical entities rather than as mathematical tools. After the quantum chromodynamics (QCD) was established, the quark model was reinforced by its successful outcome. However, while we have known that the constituent quark turned out to be different from the real elementary entity, quark, it is still an open problem to justify many of the necessary assumptions of the model[‡].

* *E-mail:* m_sakai@shirt.ocn.ne.jp

** *E-mail:* hadron-6q.hirano@hb.tp1.jp

*** *E-mail:* kato@nucl.sci.hokudai.ac.jp

† *E-mail:* y-mazda@wish.ocn.ne.jp

‡ For example, cf. Text book by F. J. Ynduráin¹

The Cotanch collaboration group proposed field-theoretic many-body approaches²⁻⁶ to hadrons around 2000. These are based on an effective Hamiltonian of the Coulomb-gauge of the QCD, and are three-dimensional but relativistic. A typical example of their effective Hamiltonian^{5,6} is of the following form;

$$H_{\text{effective}} = \int d\mathbf{x} \Psi^\dagger(\mathbf{x}) [-i\boldsymbol{\alpha} \cdot \nabla + \beta m_q] \Psi(\mathbf{x}) - \frac{1}{2} \int d\mathbf{x} d\mathbf{y} \rho^a(\mathbf{x}) V(|\mathbf{x} - \mathbf{y}|) \rho^a(\mathbf{y}) \\ + \frac{1}{2} \int d\mathbf{x} [\mathbf{\Pi}^a(\mathbf{x}) \cdot \mathbf{\Pi}^a(\mathbf{x}) + \mathbf{B}^a(\mathbf{x}) \cdot \mathbf{B}^a(\mathbf{x})] + g \int d\mathbf{x} \mathbf{J}^a(\mathbf{x}) \cdot \mathbf{A}^a(\mathbf{x}), \quad (1.1)$$

where $\Psi(\mathbf{x})$ is the quark field, and m_q is the bare quark mass, $\rho_a(\mathbf{r})$ is the color charge density;

$$\rho_a(\mathbf{r}) = \sum_{\text{flavors}} \Psi^\dagger(\mathbf{r}) \frac{1}{2} \lambda_a \Psi(\mathbf{r}) + f^{abc} \mathbf{A}^b(\mathbf{r}) \cdot \mathbf{\Pi}^c(\mathbf{r}) \quad (1.2)$$

and $V(\mathbf{x})$ is the quark-quark potential, $\mathbf{A}^a(\mathbf{x})$ is the gluon field, $\mathbf{\Pi}^a(\mathbf{x})$ is the conjugate ‘‘momentum’’ to $\mathbf{A}^a(\mathbf{x})$, and the color magnetic field, \mathbf{B}^a , is given by

$$\mathbf{B}^a = \nabla \times \mathbf{A}^a + \frac{1}{2} g f^{abc} \mathbf{A}^b \times \mathbf{A}^c. \quad (1.3)$$

Here, g is the coupling constant for quark-gluon and gluon-gluon, and $\mathbf{J}^a(\mathbf{x})$ is the quark current;

$$\mathbf{J}^a(\mathbf{x}) = \Psi^\dagger(\mathbf{x}) \boldsymbol{\alpha} \frac{1}{2} \lambda_a \Psi(\mathbf{x}). \quad (1.4)$$

Their approaches could qualitatively reproduce the charmonium mass spectrum, the π - and ρ -meson masses in the random phase approximation (RPA). However, their results are not yet final because the parameters used in the analyses are unsettled and the agreement with the experimental data is qualitative.

Llanes-Estrada-Cotanch^{2,3} and the preceding pioneers⁹⁻¹³ have tried to identify the quasiparticle mass at the small momentum with the constituent quark (CQ) mass in their quasiparticle analyses. It would be very interesting if we could discuss the constituent quark model in relation to the quasiparticle approach. In this article, we discuss the relationship between the CQ model and what we call the quasi-quark (QQ) model descended from the quasi-particle (QP) approach instead of the quasi-particle approach itself. To be specific, based on the gap equation and the Tamm-Dancoff Approximation (TDA) equation discussed in refs. [2] and [3], we derive the Schrödinger-type model equation in terms of the dynamical quark mass ($M(k)$) for a heavy quarkonium. Then treating the dynamical mass as a constant (M) and expanding the equation in $1/M$, we obtain an integro-differential equation in the configuration space that we call the quasi-quark (QQ) model equation. It is found that it is reduced to the traditional CQ model equation if a nonlocal interaction is neglected. By analyzing the charmonium S -wave states in both the models, their relationship is discussed.

We derive, in Sec. 2, the Schrödinger-type equation expressed in terms of the dynamical quark mass $M(k)$ in a QP approach studied by Llanes-Estrada and Cotanch. From the above-mentioned prescription, we obtain the QQ model equation in Sec. 3. In Sec. 4, we present our numerical results of the S -wave charmonium mass spectra using the QQ and CQ models. In Sec. 5, we give the

discussions including the e^+e^- decay widths of the charmonium states and the significance of the nonlocal interaction in particular. The last section (Sec. 6) is devoted to the concluding remarks.

2 Quasi-Particle approach by Llanes-Estrada and Cotanch

Based on the effective Hamiltonian of QCD shown in Eq. (1.1), many kinds of hadrons including constituent gluons, have been studied so far. In this work, we discuss the relationship of the QP model with the CQ model. For this purpose, we start from the following effective Hamiltonian for canonical mesons studied by Llanes-Estrada and Cotanch;^{2,3}

$$H = \int d\mathbf{x} \Psi^\dagger(\mathbf{x}) [-i\boldsymbol{\alpha} \cdot \nabla + \beta m_q] \Psi(\mathbf{x}) - \frac{1}{2} \int d\mathbf{x} d\mathbf{y} \rho^a(\mathbf{x}) v(|\mathbf{x} - \mathbf{y}|) \rho^a(\mathbf{y}), \quad (2.1)$$

where ρ_a is the color density;

$$\rho_a(\mathbf{r}) = \sum_{\text{flavors}} \Psi^\dagger(\mathbf{r}) \frac{1}{2} \lambda_a \Psi(\mathbf{r}). \quad (2.2)$$

Here, we notice that quark coupling to gluon sectors, including the hyperfine interaction is neglected for simplicity, and the Faddeev-Popov determinant is approximated by the lowest order unity. The potential $v(\mathbf{r})$ in this analysis is taken as the linear potential,

$$v(|\mathbf{x} - \mathbf{y}|) = \sigma |\mathbf{x} - \mathbf{y}|. \quad (2.3)$$

The linear plus Coulombic potential³ will be more favorable for fitting the data. The linear potential Eq. (2.3) will be suitable for qualitative investigation of how the quasi-particle model differs from the quark model.

The quark field operator $\Psi(\mathbf{x})$ is expanded in terms of the operators $B_\mu^c(\mathbf{k})$ and $D_\mu^c(-\mathbf{k})$ for quasi-particles which are related to the bare quark operators $b_\lambda^c(\mathbf{k})$ and $d_\lambda^c(\mathbf{k})$ by the Bogoliubov-Valatin transformation.^{7,8} The relationships between the two is expressed in terms of the BCS angle θ_k (or the gap angle $\phi(k)$);

$$\begin{cases} B_\mu^c(\mathbf{k}) = \cos(\theta_k/2) b_\mu^c(\mathbf{k}) - \mu \sin(\theta_k/2) d_\mu^{c\dagger}(-\mathbf{k}) \\ D_\mu^c(-\mathbf{k}) = \cos(\theta_k/2) d_\mu^c(-\mathbf{k}) + \mu \sin(\theta_k/2) b_\mu^{c\dagger}(\mathbf{k}). \end{cases} \quad (2.4)$$

The spinors transform as follows, corresponding to Eq. (2.4);

$$(U_\lambda(\mathbf{k}), V_\lambda(-\mathbf{k})) = (u_\lambda(\mathbf{k}), v_\lambda(-\mathbf{k})) \begin{pmatrix} \cos(\theta_k/2), & \lambda \sin(\theta_k/2) \\ -\lambda \sin(\theta_k/2), & \cos(\theta_k/2) \end{pmatrix}, \quad (2.5)$$

or using ϕ instead of θ_k

$$U_\lambda(\mathbf{k}) = \frac{1}{\sqrt{2}} \begin{bmatrix} \sqrt{1 + \sin \phi(k)} \chi_\lambda \\ \sqrt{1 - \sin \phi(k)} \boldsymbol{\sigma} \cdot \hat{\mathbf{k}} \chi_\lambda \end{bmatrix}, \quad V_\lambda(\mathbf{k}) = \frac{1}{\sqrt{2}} \begin{bmatrix} -\sqrt{1 - \sin \phi(k)} \boldsymbol{\sigma} \cdot \hat{\mathbf{k}} \chi_\lambda \\ \sqrt{1 + \sin \phi(k)} \chi_\lambda \end{bmatrix}. \quad (2.6)$$

By the quasi-particle spinor, the effective quasi-particle mass (dynamically generated mass) depending on the momentum transfer k is defined;

$$M(k) = k \tan \phi(k) = E \sin \phi(k) = m_q \cdot \frac{1 + \frac{k}{m_q} \tan \theta_k}{1 - \frac{m_q}{k} \tan \theta_k}. \quad (2.7)$$

And the physical vacuum $|\Omega\rangle$ satisfies the following equations;

$$B_\lambda(\mathbf{k})|\Omega\rangle = D_\lambda(\mathbf{k})|\Omega\rangle = 0. \quad (2.8)$$

It must be mentioned that although only for the quark-antiquark system, almost the same discussions as those by Llanes-Estrada and Cotanch have been done before by Orsay group,⁹⁻¹¹ S. L. Adler-A.C. Davis¹² and M. Hirata.¹³

There are two types of the QP equation of motion for the meson states, that is, TDA and RPA equations.^{2,3} In this article, we only consider the TDA equation of motion for simplicity;

$$|\Psi_{\text{TDA}}^{nJP}\rangle = Q_{nJPC}^\dagger(\text{TDA})|\Omega\rangle; \quad (2.9)$$

$$Q_{nJPC}^\dagger(\text{TDA}) = \sum_{c\mu\bar{\mu}} \int \frac{d\mathbf{k}}{(2\pi)^3} \Psi_{\mu\bar{\mu}}^{nJP}(\mathbf{k}) B_\mu^{c\dagger}(\mathbf{k}) D_{\bar{\mu}}^{c\dagger}(-\mathbf{k}),$$

$$\Psi_{\lambda\mu}^{nJP}(\mathbf{k}) = \sum_{LSm_Lm_S} \langle Lm_L Sm_S | Jm_J \rangle (-1)^{\frac{1}{2}+\mu} \langle \frac{1}{2}\lambda \frac{1}{2} - \mu | Sm_S \rangle Y_L^{m_L}(\hat{\mathbf{k}}) \psi_{LS}^{nJP}(\mathbf{k}).$$

The meson wave function $\psi_{LS}^{nJP}(k)$ in Eq. (2.9) is given by the TDA equation of motion;

$$\left\langle \Psi_{\lambda\mu}^{nJ\pi} \left| \left[H, B_\alpha^\dagger D_\beta^\dagger \right] \right| \Omega \right\rangle = (E_{nJ\pi} - E_0) \Psi_{\alpha\beta}^{nJ\pi}. \quad (2.10)$$

In the approximation neglecting mixing between different orbital angular momenta L 's, the wave function $\psi_{Ls}^{nJ\pi}(k)$ is given^{2,3} by

$$(E_{nJ\pi} - E_0 - 2\epsilon_k) \psi_{Ls}^{nJ\pi}(k) = \int_0^\infty dp \frac{p^2}{12\pi^2} K_{Ls}^{J\pi}(k, p) \psi_{Ls}^{nJ\pi}(p), \quad (2.11)$$

where ϵ_k is the expectation value of the Hamiltonian density \mathcal{H} of the physical vacuum;

$$\epsilon_k = \langle \Omega | \mathcal{H} | \Omega \rangle = kc_k + m_q s_k - \frac{2}{3} \int \frac{d\mathbf{p}}{(2\pi)^3} \hat{v}(|\mathbf{k} - \mathbf{p}|) [c_k c_p \hat{\mathbf{k}} \cdot \hat{\mathbf{p}} + s_p s_k], \quad (2.12)$$

$$(c_k \equiv \cos \phi(k), \quad s_k \equiv \sin \phi(k)),$$

and is also called the gap energy. The kernel $K_{Ls}^{J\pi}(k, p)$ for the vector mesons ($J^\pi=1^-$), which we are concerned with, is written as

$$K_{Ls}^{1-}(k, p) = 2c_k c_p \hat{v}_1 + (1 + s_k)(1 + s_p) \hat{v}_0 + (1 - s_k)(1 - s_p) \left(\frac{4}{3} \hat{v}_2 - \frac{1}{3} \hat{v}_0 \right), \quad (2.13)$$

$$\hat{v}_i \equiv \int d(\hat{\mathbf{k}} \cdot \hat{\mathbf{p}}) (\hat{\mathbf{k}} \cdot \hat{\mathbf{p}})^i \hat{v}(|\mathbf{k} - \mathbf{p}|), \quad \hat{v}(|\mathbf{k}|) = \frac{1}{2} \lim_{\mu \rightarrow 0} \frac{\partial^2}{\partial \mu^2} \frac{8\pi\sigma}{k^2 + \mu^2}. \quad (2.14)$$

The gap angle $\phi(k)$ in Eqs. (2.10)–(2.12) is given by the so-called gap equation, which determines the physical vacuum and the stationary value of the vacuum expectation value of the Hamiltonian;

$$ks_k - m_q c_k = \frac{2}{3} \int \frac{d\mathbf{p}}{(2\pi)^3} \hat{v}(|\mathbf{k} - \mathbf{p}|) [s_k c_p \hat{\mathbf{k}} \cdot \hat{\mathbf{p}} - s_p c_k]. \quad (2.15)$$

Therefore, to solve the QP equation (2.11) of motion, it is necessary to get the gap angle $\phi(k)$ by solving the gap equation (2.15) first, then to obtain the energy eigenvalue $M_{nJ\pi}$ and the corresponding wave function $\psi_{Ls}^{nJ\pi}(k)$ by substituting $\phi(k)$ in Eq. (2.11) and solving the equation.

3 Nonrelativistic Schrödinger-type quasi-particle equation in configuration space

The TDA equation of motion, Eq. (2.11), can be further rewritten to the Schrödinger-type QP equation in terms of the dynamical mass M . Noting that Eq. (2.15) is written as follows;

$$(k - U_1)s_k = (m_q - U_2)c_k, \quad (3.1)$$

$$U_1 = \frac{2}{3} \int \frac{d\mathbf{p}}{(2\pi)^3} \hat{v}(|\mathbf{k} - \mathbf{p}|) c_p \hat{\mathbf{k}} \cdot \hat{\mathbf{p}}, \quad U_2 = \frac{2}{3} \int \frac{d\mathbf{p}}{(2\pi)^3} \hat{v}(|\mathbf{k} - \mathbf{p}|) s_p,$$

the gap energy (2.12) is written as

$$\epsilon_k = (k - U_1)c_k + (m_q - U_2)s_k.$$

Using Eq. (3.1), ϵ_k is also expressed as

$$\epsilon_k = \frac{k - U_1}{c_k}. \quad (3.2)$$

From Eq. (2.7), we have

$$\epsilon_k = \sqrt{M(k)^2 + k^2} - \frac{2}{3} \int \frac{d\mathbf{p}}{(2\pi)^3} \hat{v}(|\mathbf{k} - \mathbf{p}|) c_p \hat{\mathbf{k}} \cdot \hat{\mathbf{p}} / c_k. \quad (3.3)$$

Thus, Eq. (2.11) is rewritten to be of the Schrödinger-type;

$$(E_n - E_0)\Psi_{Ls}^{nJ\pi}(k) = \left(2\sqrt{k^2 + M(k)^2} + I(k)\right)\Psi_{Ls}^{nJ\pi}(k) + \int_0^\infty \frac{dp p^2}{12\pi^2} K_{Ls}^{J\pi}(k, p) \Psi_{Ls}^{nJ\pi}(p), \quad (3.4)$$

$$I(k) \equiv -\frac{4}{3c_k} \int \frac{d\mathbf{p}}{(2\pi)^3} \hat{v}(|\mathbf{k} - \mathbf{p}|) c_p \hat{\mathbf{k}} \cdot \hat{\mathbf{p}}. \quad (3.5)$$

To observe the relationship of Eq. (3.4) with the nonrelativistic CQ model, we assume $M(k) \gg k$ and approximate the dynamical mass by a constant;

$$M(k) \rightarrow M, \quad (3.6)$$

and we take the nonrelativistic approximation of Eq. (3.4) to order $\sim 1/M$. Using the nonrelativistic expressions of s_k and c_k , we have

$$I(k) \sim \frac{4\sigma}{3k} \quad \text{and} \quad K_{Ls}^{1-}(k, p) \sim 4\hat{v}_0(k, p) \quad (3.7)$$

for the nonlocal interaction part and the kernel, respectively. From now on, we confine ourselves to the S -wave charmonium states, $L=0$, and use a simpler notation—deleting s ;

$$\Psi_{Ls}^{nJ\pi}(k) \rightarrow \Psi_{nS}(k),$$

where the suffix S stands for the S -wave. The vacuum energy E_0 is assumed to shift to E'_0 by the approximation (3.6). Then, Eq. (3.4) turns out to be

$$(E_n - E_0) \Psi_{nS}(k) = \left(2M - U + \frac{k^2}{M} + \frac{4\sigma}{3k} \right) \Psi_{nS}(k) + \frac{1}{3\pi^2} \int_0^\infty dp p^2 \hat{v}_0(k, p) \Psi_{nS}(p), \quad (3.8)$$

where $U \equiv E_0 - E'_0$.

Treating M and U as free parameters, we call a model based on this equation for the heavy quarkonium as the Quasi-Quark(QQ) model. Performing the Fourier transformation

$$\Psi_{nS}(\mathbf{r}) = \frac{1}{(2\pi)^3} \int d^3\mathbf{k} e^{i\mathbf{k}\cdot\mathbf{r}} \Psi_{nS}(\mathbf{k}), \quad (3.9)$$

the final form of the QQ model equation is obtained;*

$$M_{nS} \Psi_{nS}(r) = \left(2M - U - \frac{1}{M} \nabla^2 + \frac{4}{3} \sigma r \right) \Psi_{nS}(r) - \frac{4\sigma}{3\pi r} \int_0^\infty x dx \ln \frac{|r-x|}{r+x} \Psi_{nS}(x). \quad (3.10)$$

We solve this equation numerically[†] and show the results in the next section. The last term on the right hand-side of this equation is a nonlocal interaction, that is, characteristic of the model. It comes from $I(k)$, which is the part containing the potential \hat{v} of the gap energy (Eq. (2.12)) that is the expectation value of the Hamiltonian of the physical vacuum. If we neglect the nonlocal interaction in Eq. (3.10), the equation reduces to that of the CQ model or the potential model;

$$M_{nS} \Psi_{nS}(r) = \left(2M - U - \frac{1}{M} \nabla^2 + \frac{4}{3} \sigma r \right) \Psi_{nS}(r). \quad (3.11)$$

4 Numerical analyses of the charmonium S -wave states

We report the results of our analysis of Eqs. (3.10) and (3.11) for the S -wave charmonium states. To solve the eigenvalue problem, we use the Gaussian basis

*To control the infrared divergence of $\hat{v}(|k|)$, the limit $\mu \rightarrow 0$ was taken after the integration was performed.

[†]The integral term in Eq. (3.10) has a well-defined value in the singular integral sense, despite the logarithmic divergence on the straight line $x = r$.

expansion method,¹⁴ in which the wave function is assumed to be a sum of the Gaussian functions as follows;

$$\Psi_S(r) = \sum_{i=1}^{N_{\text{base}}} c_i \phi_i(r), \quad \phi_i(r) = N_i e^{-\nu_i r^2}. \quad (4.1)$$

The range parameter ν_i is given by a geometric series as

$$\nu_i = 1/b_i^2, \quad b_i = b_1 \gamma^{i-1}. \quad (4.2)$$

The parameters b_1 , γ and N_{base} should be chosen to give the converged solution; in the present calculations, we set

$$b_1 = 0.85, \quad \gamma = 1.15 \quad \text{and} \quad N_{\text{base}} = 20. \quad (4.3)$$

By the expansion (4.1), Eqs. (3.10) and (3.11) can be easily solved as an eigenvalue problem of a matrix in a linear vector space consisting vectors whose components are the expansion coefficients ($c_1, \dots, c_{N_{\text{base}}}$) of the Gaussian functions ϕ_i 's.

In the QQ model, there are three parameters; the dynamical quark mass M , the string tension σ , and the constant energy parameter U . As our purpose of the present work is to see whether the QQ model could be an effective model of the QP approach and to understand the relationship between the QQ model and the CQ model, we intended to perform our numerical analyses rather qualitatively.

To see the relationship between the QQ model and the QP approach, we chose the same $\sigma=0.18 \text{ GeV}^2$ used in the QP approach analysis of refs. [2] and [3] which our framework is based on. The parameter U was determined so as to bring the $1S$ mass given in ref. [3] when the dynamical c -quark mass M was fixed. The M parameter was not in the QP approach, but we noted that the bare c -quark mass $m_c=1.2 \text{ GeV}$ was there. Taking M larger than m_c but as a free parameter, we found that $M=1.4 \text{ GeV}$ could give a fit of the charmonium mass spectrum similar to the one obtained by the QP approach.

For our latter purpose to observe the relationship between the QQ model and the CQ model, and to compare their predictions with the experimental data, we adopted $\sigma=0.14 \text{ GeV}^2$ which corresponds to the quark potential fit at large distance by lattice gauge calculations^{15,16} and was used in refs. [4] and [5]. As for the dynamical mass M , we used $M=1.4 \text{ GeV}$, which was obtained in the above argument for the former of our purposes. The same values of σ and M were used both for the QQ and CQ models. The U parameter was chosen depending on each model to fit the experimental $1S$ mass data.

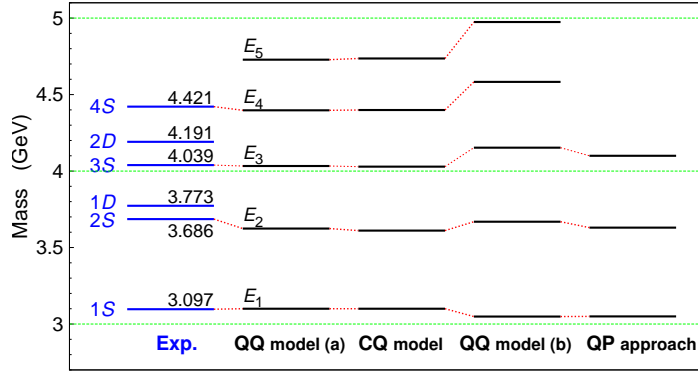
The numerical results of the charmonium mass analyses are shown together with the experimental data¹⁷ in Table 1 and in Fig. 1. The result obtained by the QQ Model (a) agrees well with the observed data and the CQ model result, and performs better than the QQ Model (b). While, the QQ Model (b) using parameters corresponding to the QP approach of refs. [2] and [3] gives a result quite similar to the QP approach result. So, we may conclude that the QQ model can be an effective model reflecting the characteristics of the QP approach.

Table 1. The charmonium mass spectra (M_{nS} in GeV)

nS	Data ¹⁷	QQ model(a)	CQ model	QQ model(b)	QP approach [‡]
		$\sigma=0.14: M=1.4$ $U=0.765$	$\sigma=0.14: M=1.4$ $U=0.383$	$\sigma=0.18: M=1.4$ $U=1.01$	$\sigma=0.18: m_c=1.2$
4S	4.421±4	4.40	4.40	4.58	
3S	4.039±1	4.03	4.03	4.15	~ 4.10
2S	3.686±0.06	3.62	3.61	3.67	~ 3.63
1S	3.097±0.006	3.10(input)	3.10(input)	3.05(input)	~ 3.05

The string tension σ is in GeV^2 ; M , m_c and U are in GeV.

[‡]The mass predictions by Cotanch *et al.*³ are given only in figures but not in numbers, and so, we have assumed the numbers by the eye from the figure.

**Figure 1.** Comparison of mass spectra for the charmonium S -wave states

5 Discussions

As shown in Table 1, the two sets; (a) and (b) for the QQ model parameters were used. From now on, we refer to the QQ model applying the set (a) simply as the QQ model and discuss the consequences since it reproduces the observed mass much better than the QQ model using set (b).

To examine and discuss the role of the nonlocal interaction in the QQ model, we consider the following equation in which a switching parameter f is introduced at the front of the nonlocal interaction term in Eq. (3.10);

$$M_{nS}\Psi_{nS}(r) = \left(2M - U - \frac{1}{Mr} \frac{d^2}{dr^2} r + \frac{4}{3}\sigma r\right)\Psi_{nS}(r) - f \frac{4\sigma}{3\pi r} \int_0^\infty x dx \ln \frac{|r-x|}{r+x} \Psi_{nS}(x). \quad (5.1)$$

For every value of f between 1 and 0, we have solved Eq. (5.1), and evaluated the expectation values of the kinetic energy $T \equiv -\frac{1}{Mr} \frac{d^2}{dr^2} r$, the linear potential $V(r) = (4/3)\sigma r$, and the nonlocal interaction term, which are represented by $\langle T \rangle$, $\langle V \rangle$ and $\langle NLI \rangle$, respectively. In Fig. 2, the f -dependences of $\langle T \rangle$, $\langle V \rangle$, $\langle NLI \rangle$ and the charmonium mass M_{nS} are shown, and in Table 2, their respective numerical values and the ratio $\langle V \rangle / \langle T \rangle$ are presented for the $f=1$ case corresponding to

the QQ model.

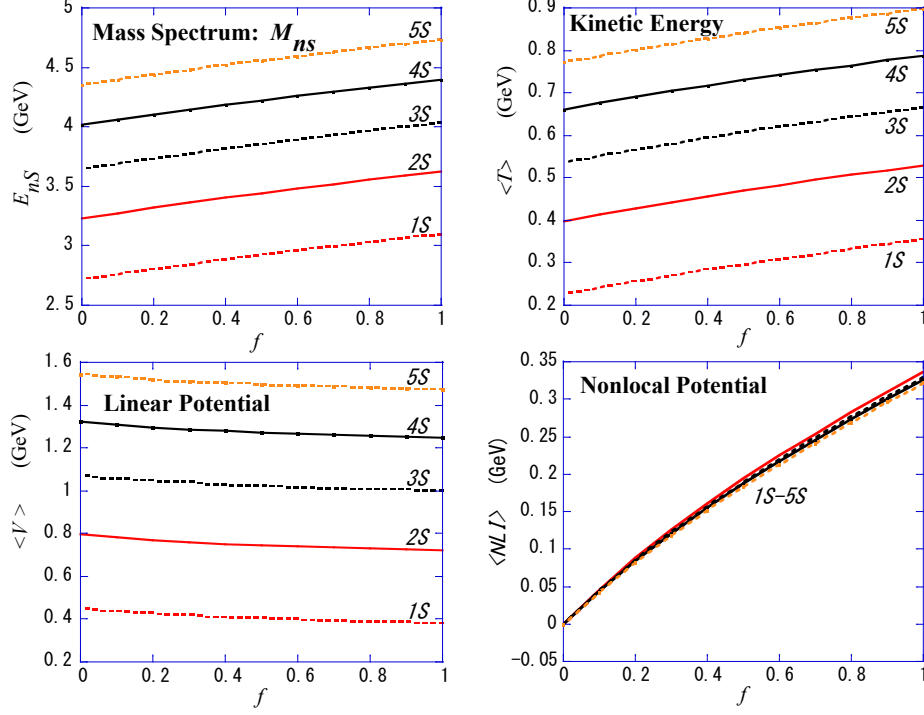


Figure 2. The f -dependences of the mass spectrum M_{nS} and the expectation values of energy terms for the S -wave $J^{PC} = 1^{--}$ charmonium states ($\sigma = 0.14 \text{ GeV}^2$ and $M=1.4 \text{ GeV}$)

Table 2. Expectation values (in GeV) of terms in Eq. (3.10) by the QQ model fit and the ratio $\langle V \rangle / \langle T \rangle$

	$\langle T \rangle$	$\langle V \rangle$	$\langle NLI \rangle$	E_n	$\langle V \rangle / \langle T \rangle$
5S	0.898	1.473	0.322	4.728	1.64
4S	0.787	1.248	0.326	4.397	1.59
3S	0.666	1.002	0.330	4.033	1.50
2S	0.530	0.723	0.336	3.624	1.36
1S	0.355	0.382	0.328	3.100	1.08

As seen in Fig. 2, the kinetic energy term increases as f increases, while the linear potential term decreases. Roughly speaking, the increase in the kinetic energy term and the decrease in the linear potential term compensate for each other, so the total energy increases by about the same amount as the increment of the nonlocal interaction term. Figures 3 and 4 demonstrate the behavior of the wave functions of the nS states for $n=1-5$ in case of $f=1$ (the QQ model) and $f=0$ (the CQ model). The wave functions behave similarly in both cases, but we find two noticeable differences; the amplitudes at the origin and numbers of

the oscillation. As seen from Fig. 3, the amplitudes at the origin are the same in the case of $f=0$ while they are different, especially showing the large amplitude for the $n=1$ state, in the case of $f=1$. From Fig. 4, we also see that the number of nodes in every nS state wave function increases by one due to the nonlocal interaction. These features show that the nonlocal interaction works attractively in a small distance region.

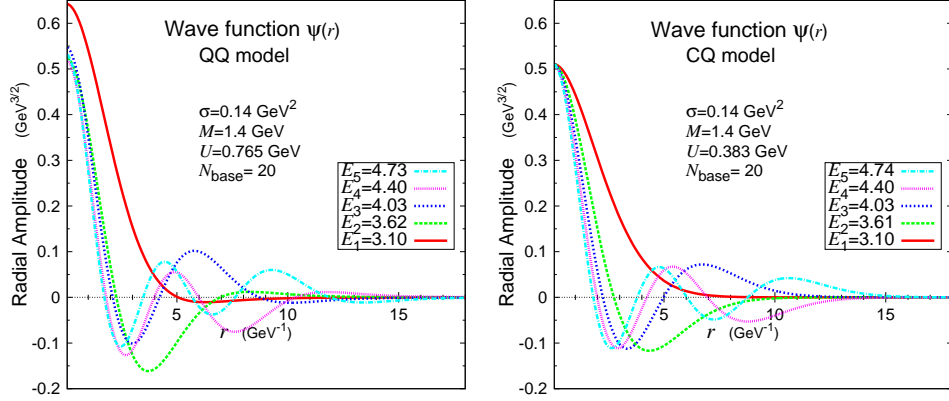


Figure 3. The radial wave function $\psi(r)$ in the cases of QQ model and CQ model

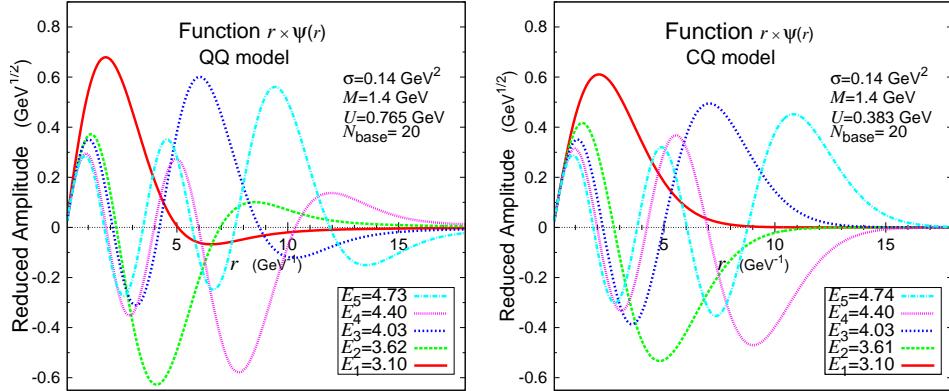


Figure 4. The reduced radial amplitude $r\psi(r)$ in the cases of QQ model and CQ model

To see more details about the effects of the nonlocal interaction, let's direct our attention to the two quantities[‡], the ratio $\langle V \rangle / \langle T \rangle$ and the values of the wave functions at the origin. In the case of $f=0$ (the CQ model), there is the so-called virial theorem^{19,20} relating the expectation value of the potential to that of the kinetic energy;

$$2\langle T \rangle|_{f=0} = \langle \mathbf{r} \cdot \text{grad } V \rangle|_{f=0}, \quad (5.2)$$

[‡]As another possible example of a physical quantity related to the wave function of the heavy quarkonium, a picture for the open flavor decays has been proposed.¹⁸

and for the linear confining potential we obtain;

$$\langle V \rangle / \langle T \rangle \Big|_{f=0} = 2. \quad (5.3)$$

In the case $f \neq 0$, the theorem does not hold. The ratio $\langle V \rangle / \langle T \rangle$, however, is expected to be not far from 2 when the effect of the nonlocal interaction is not large. Table 2 shows that the largest deviation of the ratio from 2 is for the 1S state among the five low-lying S-wave states.

As another possibility of checking these nonlocal interaction effects, we study the width of the decay of the nS state to e^+e^- . The formula for the lepton pair decay width taking the one gluon exchange correction is,^{21,22}

$$\Gamma(\psi_{nS} \rightarrow e^+e^-) = \frac{16\pi\alpha^2}{M_{nS}^2} Q_c^2 \left(1 - \frac{16}{3\pi}\alpha_s\right) |\Psi_{nS}(0)|^2, \quad (5.4)$$

where α is the fine-structure constant and the α_s is the corresponding quark-gluon constant. Since the nonlocal interaction has a copious effect on the amplitudes of the wave functions at the origin as shown in Fig. 3, the e^+e^- decay could be a good means to check the models. Although we do not assume the one-gluon-exchange interaction, we examine the decay widths of nS states in the ratio to the 2S state using Eq. (5.4);

$$R_n = \left(\frac{M_{2S}}{M_{nS}}\right)^2 \left|\frac{\Psi_{nS}(0)}{\Psi_{2S}(0)}\right|^2. \quad (5.5)$$

Table 3. The model estimates R_n (in $\text{GeV}^{3/2}$) using Eq. (5.5)

Model/Data	1S	2S	3S	4S
$\Psi_{CQ}(0)$	0.511	0.511	0.511	0.511
$\Psi_{QQ}(0)$	0.643	0.525	0.548	0.520
R_n (CQ model)	1.36	1	0.81	0.68
R_n (QQ model)	2.05	1	0.88	0.67
R_n (Exp. ¹⁷)	2.41±0.11	1	0.38±0.04	0.25±0.04
(Observed Γ)	(5.53±0.10)	(2.29±0.06)	(0.86±0.07)	(0.58±0.07)

R_n 's are compared with the data corresponding to $\psi(1S)$ – $\psi(4S)$ in the cases of CQ model and QQ model. Numbers shown in parentheses are the observed e^+e^- decay width in KeV.

The QQ and CQ model predictions are compared with the data in Table 3. In the case of the CQ model with the linear potential, R_n is given only by the mass ratio M_{2S}/M_{nS} because the amplitudes of the nS wavefunctions at the origin are the same as shown in the table.

The greatest difference in the amplitudes of wave functions at the origin and the values of R_n are seen for the 1S state. It is noticed that the model prediction for R_n of the 1S state is greatly improved by the inclusion of the nonlocal interaction. Thus, in either of the quantities $\langle V \rangle / \langle T \rangle$ and R_n , the nonlocal interaction

gives the biggest effect on the $\Psi(1S)$ and could contribute to the improvement of these predictions.

6 Concluding Remarks

We sum up the main points of this work. Based on the relativistic effective QCD Hamiltonian of the QP approach by Llanes-Estrada and Cotanch, a Schrödinger-type equation in the approximation of a constant dynamical quark mass was derived for a heavy quarkonium. The equation turned out to bring a nonlocal interaction beside the familiar local potential of the CQ model. Neglecting the nonlocal interaction, it becomes the usual CQ model type equation. This will give a field-theoretic basis for the CQ model.

To know the consequences of the newly obtained nonlocal interaction, we employed what we call, the QQ model using the Schrödinger-type equation in which all parameters including the dynamical quark mass are treated as free parameters. Applying the QQ and CQ models to the charmonium S wave states, we have obtained the following conclusions;

- 1) The QQ model is concluded to be an adequate and effective model of the QP approach by comparing their predictions on the charmonium mass spectrum.
- 2) The nonlocal interaction in the QQ model is partially absorbed in the constant energy parameter U in the CQ model, and the difference in the models doesn't appear in their charmonium mass predictions. However, the effects of the nonlocal interaction are seen in the model difference of the wave functions, and as a result, the QQ model performs better than the CQ model in the charmonium e^+e^- decay width predictions as a whole.
- 3) It may be noted that the predictions of the e^+e^- decay widths for the $3S$ - and $4S$ -states of the charmonium do not match the respective data in either model. Both the states being above the open channel threshold, the decaying effects may be important in such cases. Such hadronic interaction effects considering couplings with open channels out of scope in the present work and discussions are intended only for the bare charmonium states. As discussed in ref. [23], a further step must be taken to study the physical charmonium states for comparison of the theory with the experimental data at last.

References

1. Ynduráin, F. J.: p201 in *Quantum Chromodynamics; An Introduction to the Theory of Quarks and Gluons.*: Springer-Verlag 1983
2. Llanes-Estrada, F. J., Cotanch, S. R.: Phys. Rev. Lett. **84**, 1102 (2000)
3. Llanes-Estrada, F. J., Cotanch, S. R.: Nucl. Phys. A **697**, 303 (2002)
4. Llanes-Estrada, F. J., Cotanch, S. R.: Phys. Lett. B **504**, 15 (2001)

5. Cotanch, S. R.: *Fizika* **B13**, 27 (2004)
6. Llanes-Estrada, F. J., Cotanch, S. R., Szczepaniak, A. P., Swanson, E. S.: *Phys. Rev. C* **70**, 035202 (2004)
7. Bogoliubov, N. N.: *Nuovo Cim.* **7**, 794 (1958)
8. Valatin, J. G.: *Nuovo Cim.* **7**, 843 (1958)
9. Amer, A., Yaouanc, A. Le, Oliver, L., Pène, O., Raynal, J.-C.: *Phys. Rev. Lett.* **50**, 87 (1983)
10. Yaouanc, A. Le, Oliver, L., Pène, O., Raynal, J.-C.: *Phys. Rev. D* **29**, 1233 (1984)
11. Yaouanc, A. Le, Oliver, L., Ono, S., Pène, O., Raynal, J.-C.: *Phys. Rev. D* **31**, 137 (1985)
12. Adler, S. L., Davis, A. C.: *Nucl. Phys. B* **244**, 469 (1984)
13. Hirata, M.: *Prog. Theor. Phys.* **77**, 939 (1987) Valatin, J. G.: *Nuovo Cim.* **7**, 843 (1958)
14. Hiyama, E., Kino, Y., Kamimura, M.: *Progress In Particle and Nuclear Physics* **51**, 223 (2003)
15. Bali, G. S.: *Phys. Reports*, **343**, 1 (2001)
16. Kawanai, T., Sasaki, S.: *Phys. Rev. Lett.* **107**, 091601 (2011)
17. Zyla, P. A., et al.: *Prog. Theor. Exp. Phys.* **2020**, 083C01 (2020)
18. Torres-Rincon, J. M., Llanes-Estrada, F. J.: *Phys. Rev. Lett.* **105**, 022003 (2010)
19. Schiff, L. I.: *Quantum Mechanics*, p140.: McGraw-Hill 1955
20. Lucha, W., Schöberl, F. F., Gromes, D.: *Phys. Reports* **200**, No. 4 (1991) 127
21. Barbieri, R.: "Hadrons (Usual and Newly Discovered) in Gauge Theories; A Dream?" in *Weak and Electromagnetic Interactions at High Energies.*: Plenum Press 1976
22. Barbieri, R., Kögerler, R., Kunst, Z., Gatto, R.: *Nucl. Phys. B* **105**, 125 (1976)
23. Bicudo, Pedro J. de A., Ribeiro, José E. F. T.: *Phys. Rev. D* **42**, 1611 (1990)